ISSN 1063-7710, Acoustical Physics, 2011, Vol. 57, No. 4, pp. 542–550. © Pleiades Publishing, Ltd., 2011.

ACOUSTIC SIGNAL PROCESSING AND COMPUTER SIMULATION

Parameter Selection Methods of Delay and Beamforming for Cochlear Implant Speech Enhancement[1]

Qin Gong and Yousheng Chen

Dept. of Biomedical Engineering, Tsinghua University, Beijing, 100084 P.R. China

e-mail: gongqin@mail.tsinghua.edu.cn

Received August 4, 2010

Abstract—Speech acquisition by a cochlear implant (CI) is typically performed by a single omnidirectional microphone. In order to improve the signal-to-noise ratio (SNR) of sound collected from the forward direction, the delay beamforming method is applied to satisfy the size and processing limitations. The optimal delay time and weighting parameters, selected by our proposed graphical method, yielded a beam pattern that strongly enhanced speech from the front, while noise from lateral and rear directions were sharply weakened, making the method appropriate for use in CI applications.

DOI: 10.1134/S106377101104018X

INTRODUCTION

The performance of cochlear implant (CI) devices has improved greatly over the past ten years, allowing users to communicate in face-to-face and phone conversations. However, speech recognition in noisy environments remains poor [1–3]. Most devices currently in clinical use are equipped with a single omnidirectional microphone, and the utilization of two or more microphones remains in the research stage. The microphone array method promises to be an effective way to improve CI speech recognition performance, particularly for situations in which the desired voice signal and ambient noise originate from different directions.

Due to the small size of CI products [4], the number of onboard microphones is limited. In this paper, a dual-microphone array that meets the requirements for CI devices was adapted for front-end speech enhancement. Several beamforming methods for speech enhancement have been presented previously in the literature, such as delay beamforming [5, 6], adaptive null-forming [7–9] and the complex method of combining filters [10–13]. The delay beamforming method was adopted due not only to limitations in the physical size of CI devices, but also their computational speed. The desired beam pattern was obtained by adjusting algorithm delay time and weighting factor, while adhering to the needs of low calculation in real-time speech processing.

[1] The article is published in the original.

METHOD OF DELAY BEAMFORMING AND DESIGN SPECIFICATIONS

Method of Beamforming with Dual Omnidirectional Microphones

A schematic drawing for the delay beamforming method with dual omnidirectional microphones is illustrated in Fig. 1. MIC_1 and MIC_2 represent two microphones separated by 1 cm, a practical distance for many CI devices.

In Fig. 1, using a counter-clockwise notation, the speech source is to the right (forward direction = 0°), 180° indicates a rear-facing orientation, then 90° and 270° are lateral directions. τ and β, respectively, are the delay time and weighting parameters for the rear microphone MIC_2, and θ is the angle between the sig-

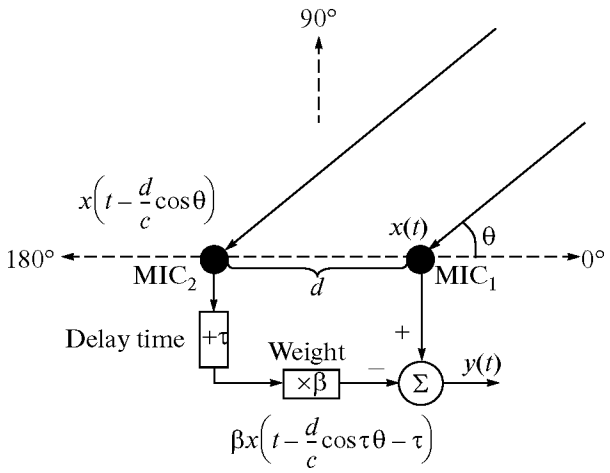

Fig. 1. Delay beamforming method with dual omnidirectional microphones.

nal and the forward direction. If we denote the signal obtained by MIC_1 as $x(t)$, then the signal obtained by microphone MIC_2 can be described as $x(t - \frac{d}{c}\cos\theta)$. The recorded signal in MIC_2 after the signal is appropriately delayed (τ) and weighted (β), is $\beta x(t - \frac{d}{c}\cos\theta - \tau)$, where c was the speed of sound. Thus, the total system output is described by Eq. (1):

$$y(t) = x(t) - \beta x\left(t - \frac{d}{c}\cos\theta - \tau\right), \quad (1)$$

where $\frac{d}{c}$ represents the sound propagation time for the inter-microphone distance d. To facilitate the analysis, the algorithm delay can be written as $\tau = k\frac{d}{c}$, where the coefficient k is defined as a ratio of the delay time and the time required for sound to traverse the distance $\frac{d}{c}$ between the microphones. Then, the output signal $y(t)$ can be expressed as Eq. (2):

$$|H(e^{j\omega})| = \left|1 - \beta e^{-j2\pi f\frac{d}{c}(\cos\theta + k)}\right|, \quad (2)$$

In Eq. (2), f is the signal frequency, and the magnitude response $|H(e^{j\omega})|$ changes as a function of the signal direction θ and generates the directional enhancement effect.

Requirements of CI Users for Speech Enhancement and the Design Specifications of the Beam Pattern

To listen to a voice in a noisy environment, CI users need to filter out non-speech signals arriving from directions other than that of the speaker. Some studies have proposed an adaptive null-forming algorithm to reduce noise in hearing-aid applications [7, 14–16]. This method can adaptively suppress the noise from certain directions, but requires large calculation, which exceeds the capability of current CI devices. Therefore, the delay beamforming method, with minimal computational complexity in microphone array techniques, is adopted in this paper.

During a conversation for CI users, the forward-direction sound must be heard clearly, with less attention paid to sound from lateral and rear directions. Hence, the required beam pattern should have maximal response in the front-facing direction, followed by the lateral direction, and a minimal output for noise emanating from a backwards-direction. In addition, larger contrast between the signals from these orientations is more desired. Specifically, minimum design specifications for CI devices generally require the forward-direction response to be 3 and 5 dB larger than lateral and rear directions, respectively. Also, if the response at a certain direction changes too rapidly, the user may experience strong discomfort. Therefore, a suitable beam pattern should possess a response that decreases smoothly and monotonically as the source moves from the forward to rear in order to generate a comfortable listening environment.

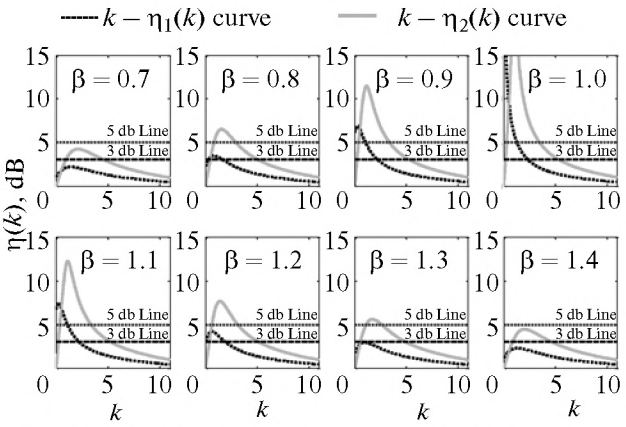

Fig. 2. $k - \eta_1(k)$ and $k - \eta_2(k)$ curves using various values of β.

PARAMETER SELECTION ALGORITHM

Method of Adjusting the Delay Time Based on a Fixed Weighting Factor

In this paper, $\eta_1(k)$ is used to indicate the ratio of the system magnitude response at 0° to that of the 90° (lateral) direction, and $\eta_2(k)$ indicates the same ratio when compared to the 0° and 180° directions (both in dB). By applying Eq. (2), $\eta_1(k)$ can be expressed as:

$$\eta_1(k) = 20\log\left(\left|\frac{H(e^{j\omega})|_{0^\circ}}{H(e^{j\omega})|_{90^\circ}}\right|\right) = 20\log\left|\frac{1 - \beta e^{-j2\pi f\frac{d}{c}(1+k)}}{1 - \beta e^{-j2\pi f\frac{d}{c}k}}\right|. \quad (3)$$

Similarly, $\eta_2(k)$ can be written as:

$$\eta_2(k) = 20\log\left|\frac{1 - \beta e^{-j2\pi f\frac{d}{c}(1+k)}}{1 - \beta e^{-j2\pi f\frac{d}{c}(-1+k)}}\right|. \quad (4)$$

Since the primary energy and information carrying frequencies of speech are concentrated in a range centered around 1000 Hz. Values representing actual designs parameter (f = 1000 Hz, d = 0.01 m, c = 340 m/s) can be substituted into Eqs. (3) and (4), with β and k remaining as undetermined quantities. Increasing β in increments of 0.1 yields the $k - \eta(k)$ curves shown in Fig. 2.

Fig. 2 presents the $k - \eta_1(k)$ and $k - \eta_2(k)$ curves for various weighing factors; in every case both curves possess distinct peaks. In order to comply with the design specifications that $\eta_1(k)$ exceed 3 dB and $\eta_2(k)$ exceed 5 dB, we have the constraint that the weighting

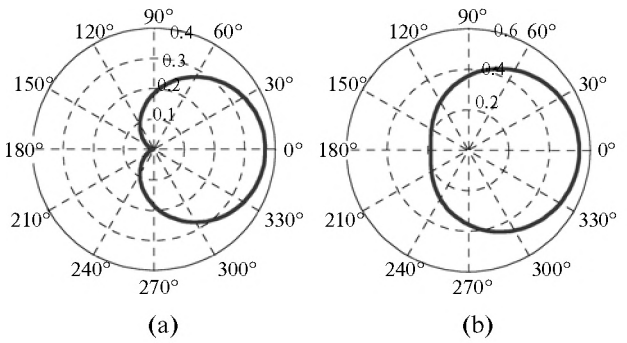

Fig. 3. Beam pattern using weight $\beta = 1$ and the delay ratio (a) $k = 1$, (b) $k = 2$.

factor must be in the range $0.8 < \beta < 1.3$, and the optimal value of the delay ratio should be evaluated in this range.

The value of k that maximizes the $k - \eta_1(k)$ curve does not coincide with the optimal value of k in the $k - L\eta_2(k)$ curve. Since $k - \eta_2(k)$ is steeper, the optimal delay ratio k can be obtained near the peak of $k - \eta_2(k)$ curve.

When using weighting factors of $\beta = 0.8$, 0.9, 1.1, 1.2, 1.3, all of these corresponding beam patterns at the peak of the $k - \eta_2(k)$ curve met the design requirement of smoothness at all orientations and a monotonic decrease moving from the forward to lateral to rear directions. A special case is $\beta = 1$, the corresponding beam pattern at the peak of $k - \eta_2(k)$ curve does not satisfy the condition of smoothness (Fig. 3a), the delay ratio k must be adjusted to $k = 2$ (Fig. 3b).

The optimal value of the delay ratio k at each weight β and corresponding $\eta_1(k)$ and $\eta_2(k)$ are listed in Table 1.

Comparison of $\eta_1(k)$ and $\eta_2(k)$ at each optimal parameter occur at weighting factor $\beta = 1.1$ and $k = 1.1$ (corresponding to a delay time $\tau = 1.1\ d/c$, or 32 μs under actual application conditions and $d = 0.01$ m). The resulting values of $\eta_1(k)$ and $\eta_2(k)$ are 5.0 and 12.2 dB respectively. Thus, the response at the forward direction is about 5 and 12 dB larger than those in lateral and rear directions, respectively.

Table 1. The optimal delay ratio and corresponding beam pattern specifications at each weight

Weight β	Optimal delay ratio k	$\eta_1(k)$	$\eta_2(k)$
0.8	1.54	3.1	6.5
0.9	1.14	4.8	11.5
1.0	2	3.5	9.4
1.1	**1.1**	**5.0**	**12.2**
1.2	1.4	3.6	7.7
1.3	1.66	3.7	5.7

Method of Adjusting the Weighting Factor Based on a Fixed Delay Time

Increasing the delay ratio k in increments of 0.1 yields the $\beta - \eta(k)$ curves shown in Fig. 4.

Figure 4 presents the $\beta - \eta_1(k)$ and $\beta - \eta_2(k)$ curves for various values of the delay ratio k. When $k < 0.6$, the $\beta - \eta_1(k)$ curve is above the $\beta - \eta_2(k)$ curve, indicating that the lateral-direction signal is weakened more than the rear-direction signal. This does not satisfy the design specification of monotonicity. When $k > 2.3$, the peak of the $\beta - \eta_1(k)$ curve is below the 3 dB line for all weights β. Therefore, the suitable range of the delay ratio is $k = (0.6, 2.3)$.

Fig. 4 also shows that the peaks of the $\beta - \eta_1(k)$ and $\beta - \eta_2(k)$ curves occur at the same weight value, $\beta = 1$. Since the beam pattern does not satisfy the conditions of smoothness and monotonicity at exactly $\beta = 1$, the optimal weights β are close to 1, with a small offset. In Fig. 4, for $k = 0.9$ 1.0, 1.1, the peak values of the $\beta - \eta_1(k)$ and $\beta - \eta_2(k)$ curves were clearly much larger than the others, so it is only necessary to consider these values, along with their corresponding beam patterns.

In Fig. 5, the beam patterns marked with a grey square are found to be optimal since the weiths β are nearest to 1 at corresponding delay ratios while meeting the ctiteria of smoothness and monotonicity. When choosing $k = 0.9$, 1.0, 1.1, the corresponding weights are $\beta = [0.8, 1.2]$, $\beta = [0.9, 1.1]$ and $\beta = [0.9, 1.1]$ respectively. The values of $\eta_1(k)$ and $\eta_2(k)$ obtained in these parameters are shown in Table 2.

The values of $\eta_1(k)$ and $\eta_2(k)$ using these three values of the delay ratio and weights between 0.8 and 1.2 are illustrated in Fig. 5.

Table 2 emphasizes two sets of optimal parameters, ($k = 1.0$, $\beta = 1.1$) and ($k = 1.1$, $\beta = 1.1$), marked in grey. The first set has $\eta_1(k) = 5.2$, which is slightly larger than the corresponding $\eta_1(k) = 5.0$ of the second set. However, the tradeoff is that the $\eta_2(k)$ value of the first set, 12, is slightly smaller than the second, $\eta_2(k) = 12.2$. For most CI applications, sound coming from the rear is of little interest, so it should be weakened the most. As a result, the final choice of parameters is $\beta = 1.1$ and $k = 1.1$ corresponding to the delay time $\tau = 1.1\ d/c$.

SIMULATION RESULT

Optimal Parameters

The analyses developed in the previous two sections converged on the same optimal parameters: $\tau = 1.1\ d/c$ and $\beta = 1.1$, corresponding to $\eta_1(k) = 5.0$ and $\eta_2(k) = 12.2$. Using these values, if speech from the forward direction is the desired signal, and sound from other directions, which may include other conversations, is considered noise, these optimal parameters enhance the target speech by about 5 and 12 dB compared to the lateral and rear directions, respec-

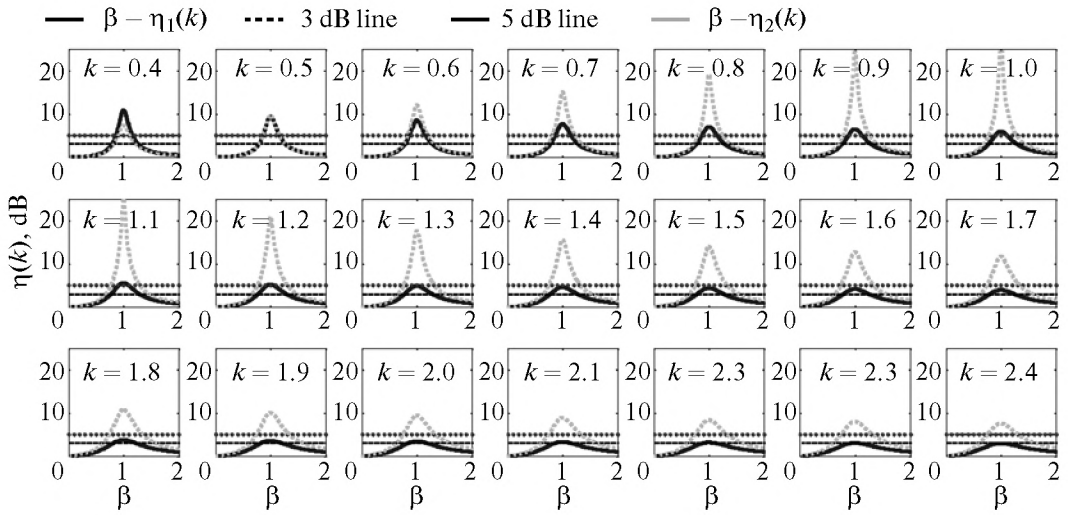

Fig. 4. $\beta - \eta_1$ and $\beta - \eta_2$ curves for different values of k.

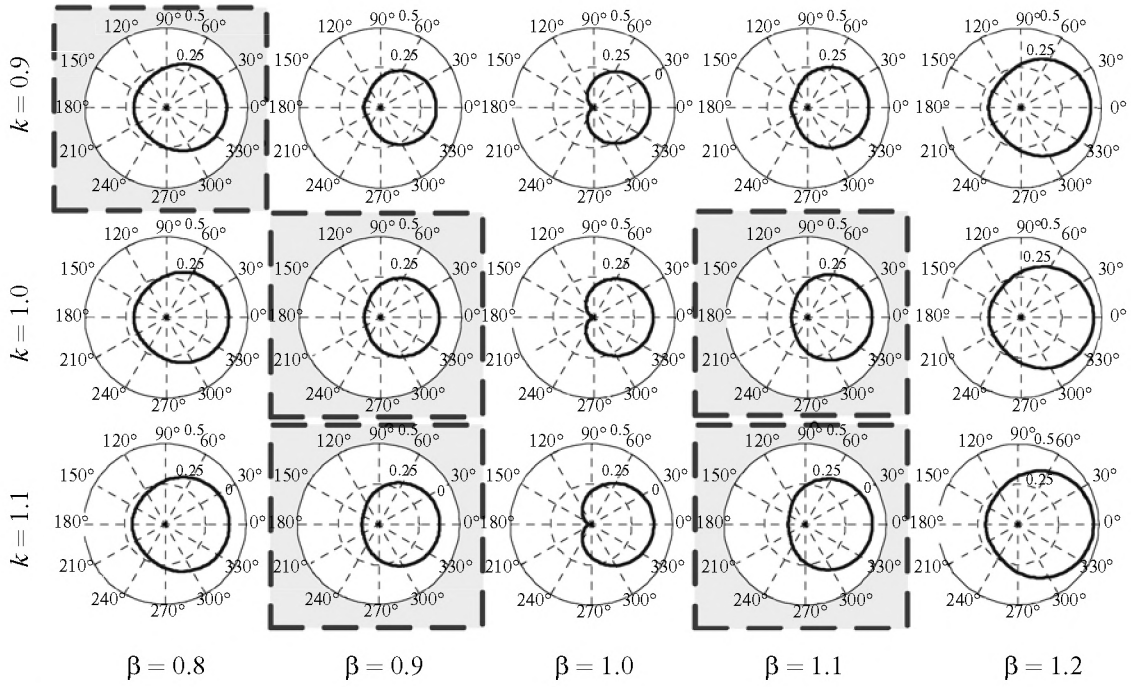

Fig. 5. The beam pattern corresponding to delay ratios $k = 0.9$, 1.0, 1.1 and weighting factor $\beta = 0.8$, 0.9, 1.0, 1.1, 1.2.

tively, and meet the requirements of smoothness and monotonicity.

Characteristics of the Optimal Beam Pattern

After selecting the optimal design parameters $\tau = 1.1\ d/c$ and $\beta = 1.1$, the corresponding beam pattern and system response for all source orientations (0° to 360°) are shown in Figs. 6a and 6b.

Using these settings, the magnitude response of the beam pattern is maximized for signals from the forward direction, minimized for noise originating in the rear, and possesses an intermediate value for lateral directions (Fig. 6a). As shown explicitly in Fig. 6b, the curve displays a smooth, monotonous decrease in magnitude as the angle moves away from 0, a minimum at π radians, and a corresponding increase as the angle completes the rotation at 2π. Thus, the designed beam pattern satisfies the design specifications, with a speech enhancement of about 5 dB over lateral directions and 12 dB over noise from the rear direction.

Table 2. Optimal weights and corresponding beam pattern specifications for each delay ratio $k = 0.9, 1.0, 1.1$

Delay ratio k	Optimal weight β	$\eta_1(k)$	$\eta_2(k)$
0.9	0.8	3.5	4.1
1.0	0.9	4.1	11.2
	1.1	5.2	12.0
1.1	0.9	4.9	11.4
	1.1	5.0	12.2

EXPERIMENTAL RESULT

Description of the Hardware Platform and Testing Method

For this paper, experimental data was recorded using a dual-microphone hardware platform for CI front-end speech enhancement (Fig. 7).

This platform used two EM omnidirectional microphones (Knowles), MIC_1 and MIC_2, held 1 cm apart by a supporting frame. The microphone modules recorded the voice signal and generated an electrical output. After the signal was sent to the hardware platform for amplification and filtering, it was then transferred to a dual-channel USB sound card. The data was then uploaded to a computer for algorithm processing.

The testing was carried out in a large room (approximately $8 \times 8 \times 4$ m). The testing method, location of the hardware platform, and the placement of the speech signal and noise are illustrated in Fig. 8.

In Fig. 8, four loudspeakers were used to produce the speech signal (1, in the forward direction) and noise (2, 3, and 4). The dual-microphone hardware platform was located in the center (point O), equidistant (1.5 m) from every source. The recorded signal, after preprocessing, amplification, and filtering, was transmitted to the corresponding left and right channels of the computer's sound card via a high-speed USB interface. The software interface was developed using Matlab 7.4, with adjustable sampling rate, time, and channel parameters, in order to control the process of data acquisition. The delay beamforming method for speech enhancement was applied to the data and the real-time processed signal was sent to the loudspeakers for playback to assess the suitability of the algorithm. Simultaneously, the data was stored on the computer's hard disk as a *.wav file for further analysis.

Testing the Directional Gain of a Narrowband Sine Signal

A narrow-band 1000 Hz sine signal was used to calculate the beam pattern in Fig. 6, and the theoretical result predicted that the lateral and rear noises would be weakened by 5 and 12 dB, respectively, compared to speech from the forward direction. In this test, a 1000 Hz sine signal was played for one second from the forward, lateral and rear positions (1, 2, and 4 in Fig. 8), at the same volume, by three loudspeakers in turn. The dual-microphone array recorded the signal illustrated in Fig. 9.

The sub-figure 9a shows the recorded sounds of the 1000 Hz sine signals from the the forward, lateral and rear directions. The amplitudes were very nearly equal, consistent with the characteristics of an omnidirectional-microphone. Fig. 9b displays the signal waveform after processing with the delay beamforming method using the parameters $\tau = 1.1\ d/c$ and $\beta = 1.1$. The relative time-averaged amplitudes in the forward, lateral and rear directions were about 1 : 0.6 : 0.3, corresponding to approximate reductions of 4.4 and 10.5 dB in the lateral and rear signals, respectively. Thus, the test results closely matched the theoretical

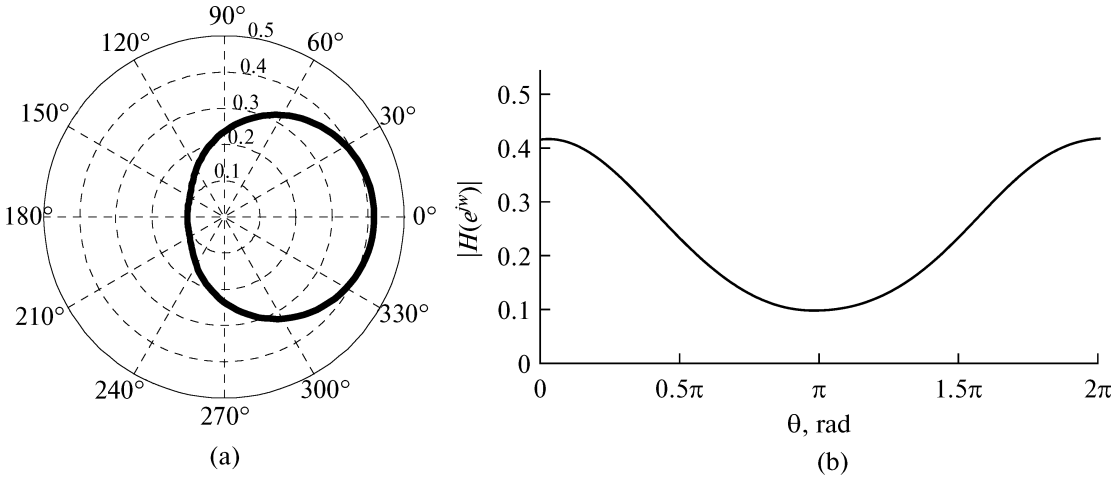

Fig. 6. (a) The beam pattern corresponding to delay time of $\tau = 1.1\ d/c$ and weighting factor $\beta = 1.1$; (b) the system response at all orientations using these parameters.

predictions of a 5 and 12 dB reduction of the lateral and rear signals, which would have yielded amplitude ratios of about 1 : 0.56 : 0.25.

Testing Speech Enhancement in a Noisy Environment

For this test, a speech signal (using English word *"beautiful"* as material, played twice) was acquired from the forward direction while loudspeakers played noise (the theme song from the movie *Titanic*, "My heart will go on") in the forward, lateral and rear directions, sequentially. The recorded signals after enhancement are shown in Fig. 10.

Figure 10 illustrates the speech signal with musical noise from each of the three directions (forward, lateral and rear), recorded by the hardware platform. Comparison of the sub-figures (a), (b) and (c) reveals that the volume of the speech signal coming from the front was the same each time (inside the two pairs of dashed lines), while the lateral and rear music signals (the noise) are sharply weakened. The relative average amplitudes of the noise in these cases are found to be about 1 : 0.63 : 0.35, corresponding to a SNR increase of 4 and 9 dB for the lateral and rear directions, respectively, consistent with the theoretical results.

Experiments Regarding the Influence of the Head

The external part of a cochlear implant consists primarily of the microphone and speech processor. Types of microphone commonly in use include BTE (behind the ear), ITC (in the cannal), ITE (in the ear) and CIC (completely in the cannal) configurations. The signal acquisition of all these microphones may be affected by the user's head, while the influence of other parts of the body can be ignored. In this experiment, an acoustic phantom in the shape of a human head was used to test its effect on CI signal acquisition (Fig. 11).

In Fig. 11, the hardware platform was placed on the model's left side. The dual microphones were set at the center (point O), collinear with the ear canal (about 2 cm away). The speakers were again placed 1.5 m from the microphones, arranged in a circle, with 36 testing positions spaced at 10° intervals. Each speaker played a 3-pulse sinusoidal signal (1000 Hz, 1 s pulse duration with 2 second intervals) in turn, once with the phantom present, and then again with it removed. Meanwhile, the platform recorded the signal in real-time. Fig. 12 shows the recorded waveform for the speaker at the 0° position with and without the phantom.

After each test, the average signal amplitude were recorded. The test was repeated with the microphone placed on the model's left side.

Figure 13 indicates the beam pattern of the free acoustic field (marked by the circle) and the beam pattern in the presence of the model (marked by the triangle). Without the phantom, the response in all

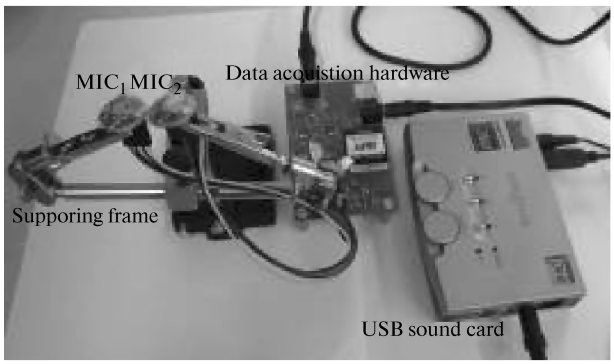

Fig. 7. Dual-microphone hardware platform for CI front-tend speech enhancement.

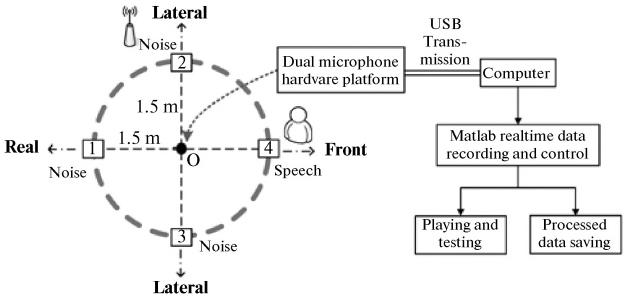

Fig. 8. The testing method and data processing flow chart.

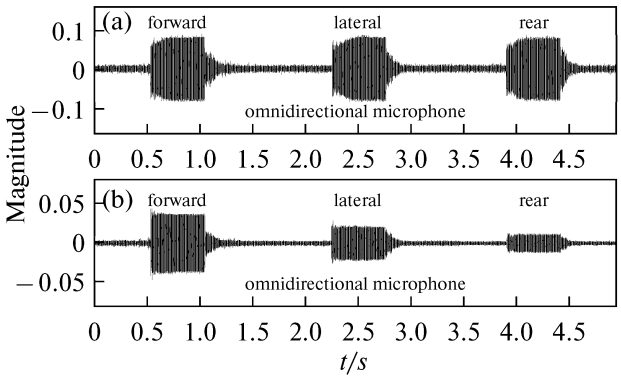

Fig. 9. Testing of a 1000 Hz sine signal. (a) Recorded results in an omnidirectional microphone. (b) Results after delay beamforming based on optimal parameters.

directions was nearly the same, consistent with expectations. That is, the omnidirectional microphone has the same sensitivity in all directions. However, the presence of the head phantom significantly affected the signal acquisition of the omnidirectional microphone. When the microphone was placed on the model's left side, as shown in Fig. 13a, the beam pattern changed noticeably in the 180°–359° region, with a "shadowing" effect leading to a smaller average amplitude compared to the results in the free acoustic field. This clearly demonstrates that the head can

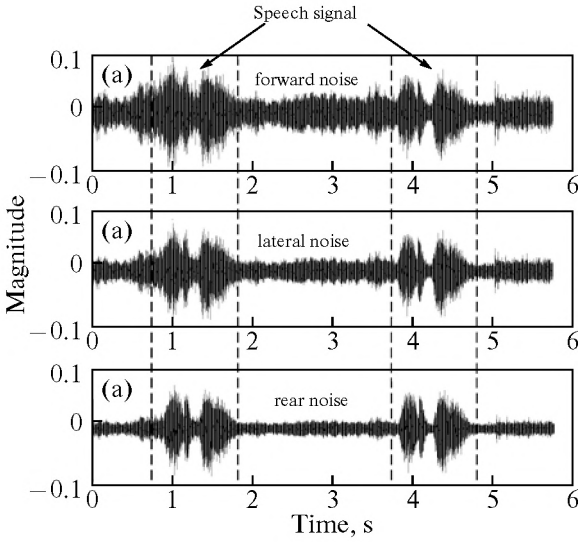

Fig. 10. Testing speech enhancement in the presence of noise in the form of background music. (a) Noise coming from the front; (b) Noise coming from the side; (c) Noise coming from the back.

noticeably influence the omnidirectional sensitivity characteristics of the signal acquisition. Opposite the phantom, in the 0°–180° orientation range, the average amplitude was slightly larger than in the free acoustic field, with the same sensitivity in this range. That is, sounds originating from the side without the acoustic shadow maintained their omnidirectional characteristics. When the microphone was placed on the model's right side (Fig. 13b), an analogous, but mirror-reversed result was obtained, as expected.

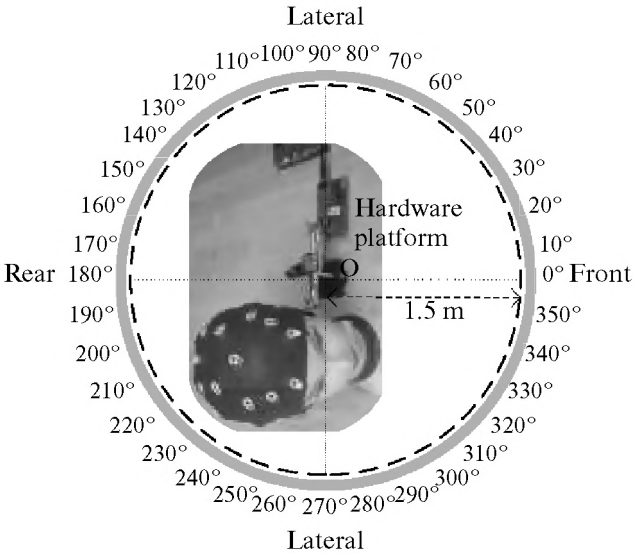

Fig. 11. Hardware setup and testing method for the experiments on the acoustic influence of the head.

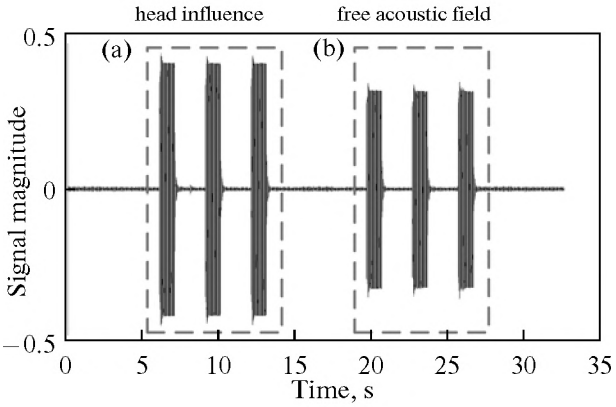

Fig. 12. The recorded signal from the omnidirectional microphone at the 0° position (a) with and (b) without presence of the acoustic phantom.

Therefore, by analyzing Fig. 13, the following conclusion can be drawn for signal acquisition by an omnidirectional microphone: the side containing the head model will experience an acoustic shadow that will reduce the amplitude of sounds coming from that direction; while the other side, with the same sensitivity in this range, will produce a larger amplitude, possibly due to reflections from the phantom. Using the proposed speech enhancement method with optimal parameters ($\tau = 1.1\ d/c$ and $\beta = 1.1$), and the signals recorded by the dual-microphone hardware platform, the beam patterns of Fig. 14 were produced.

In Fig. 14, the theoretical beam patterns discussed in the previous sections are marked by dotted line. In the free acoustic field, the testing results (marked by circle) indicate the actual directional sensitivity was slightly weakened, with the forward amplitude about 4.4 and 10.5 dB larger than those at lateral and rear directions, respectively. This sensitivity, as well as the smoothness and monotonicity of the beam pattern, makes this method attractive for CI applications. When the microphone was placed on the model's left side (Fig. 14a), the amplitude trace (marked by the triangle) indicates that the the beam pattern for angles in the range of 180°–359° orientation was essentially the same as that of the free acoustic field, and only a 3 dB deviation was found in the range that included the model (200°–250°). The average amplitude in the 0°–180° orientation, opposite the model, was slightly larger than for the free acoustic field, but remains the same directivity sensitivity in this range. The test results show that the shadow formed by the acoustic phantom can affect the beam pattern slightly when using parameters optimized for the free field, but the output remains within an acceptable error range. In total, the effect of the head phantom was less than 10% compared to the case in the free acoustic field. Therefore, the speech enhancement method introduced here should be considered robust enough to work even after the acoustic shadow of the head is included.

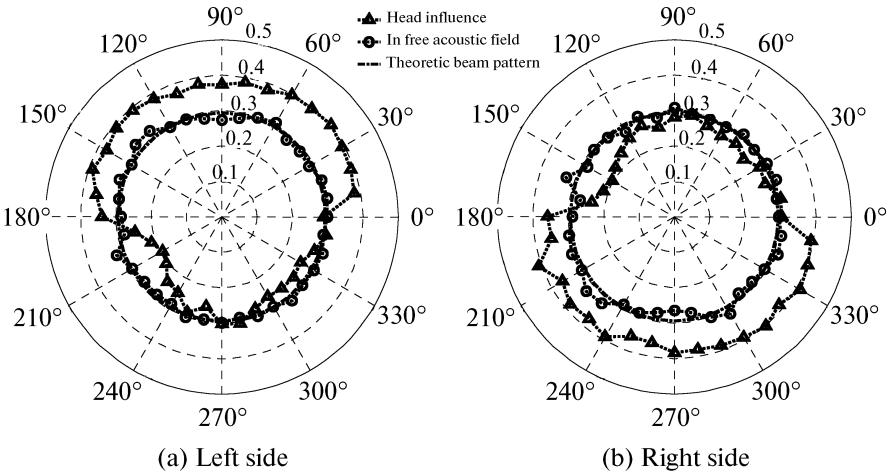

Fig. 13. The beam pattern from an omnidirectional microphone. The red trace is from the free acoustic field, without the phantom present. The blue traces show the corresponding amplitudes when the microphone is placed on the model's (a) left and (b) right side.

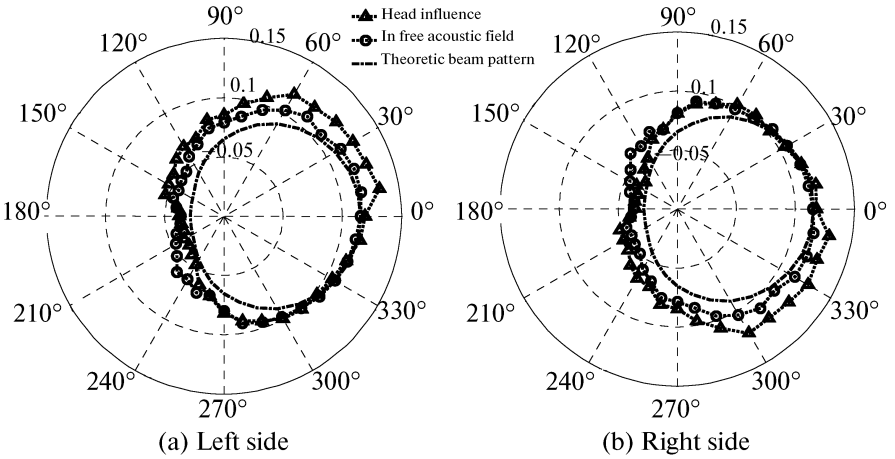

Fig. 14. Measured beam pattern using the optimal parameters in the presence of the acoustic phantom compared with the free acoustic field when the microphone is placed on the model's (a) left and (b) right side.

CONCLUSIONS

The proposed graphical method of parameter selection to find the optimal delay time and weighting parameters for a dual-microphone delay beamforming device yielded an actual speech enhancement of 4 and 9 dB for signal in the forward direction relative to those in lateral and rear directions, respectively. And the experimental results for acoustic shadow of the head indicate this method is robust. These chosen parameters, suitable for CI applications, could help improve speech recognition by users in noisy environments.

ACKNOWLEDGMENTS

This work was supported by the National Natural Science Foundation of China under the grant nos. 60871083 and 30800234, by Beijing Natural Science Foundation under the grant no. 3082012, by the Key Technologies R&D. Program of Ministry of Science and Technology of the People's Republic of China under the grant no. 2008BAI50B08.

REFERENCES

1. G. S. Stickney and F. G. Zeng, J. Acoust. Soc. Am. **116**, 1081 (2004).
2. G. P. Li and M. E. Lutman in *Proceedings of the 16th European Signal Procession Conference* (Lausanne, Switzerland, 2008).
3. K. Chung and F. G. Zeng, Hear. Res. **250**, 27 (2009).
4. B. S. Wilson and M. F. Dorman, J. Rehabil. Res. Dev. **45**, 695 (2008).
5. J. L. Flanagan, J. Acoust. Soc. Am. **78**, 1508 (1985).

6. W. Kellermann, in *Proceedings of IEEE International Conference on Acoustics, Speech, and Signal Processing* (Toronto, Canada, 1991), vol. 5, pp. 3581–3584.
7. F. L. Luo, J. Yang, and C. Ppavlovic, IEEE T. Audio Speech **50**. 1583 (2002).
8. B. Zhang, Ch. Wang, and M. Lu, Acoust. Phys. **49**, 688 (2003).
9. A. A. Mal'tsev, R. O. Maslennikov, A. V. Khoryaev, and V. V. Cherepennikov, Acoust. Phys. **51**, 195 (2005).
10. R. Zelinski, in *Proceedings of IEEE International Conference on Acoustics, Speech, and Signal Processing* (New York, NY, USA, 1988), pp. 2578–2581.
11. F. Khalil, J. P. Jullien, and A. Gilloire, J. Audio Eng. Soc. **42**, 691 (1994).
12. T. Chou, in *Proceedings of IEEE International Conference on Acoustics, Speech, and Signal Processing* (Detroit, MI, USA, 1995), vol. 5, pp. 2995–2998.
13. J. S. Marciano and T. B. Vu, Electron. Lett. **36**, 682 (2000).
14. P. M. Peterson, N. I. Durlach, W. M. Rabinowitz, and P. M. Zurek, J. Rehabil. Res. Dev. **24**, 103 (1987).
15. M. Kompis and N. Dillier, J. Acoust. Soc. Am. **109**, 1134 (2001).
16. F. Kuk, D. Keenan, C. C. Lau, and C. Ludvigsen, J. Am. Acad. Audiol. **16**, 333 (2005).